

## Research Article

# Silencing the ADAM9 Gene through CRISPR/Cas9 Protects Mice from Alcohol-Induced Acute Liver Injury

Yong-Yong Zhang <sup>1,2,3</sup>, San-Qiang Li <sup>1,3</sup>, Ying Song<sup>1,3</sup>, Ping Wang <sup>1,3</sup>, Xiao-Gai Song<sup>1,3</sup>, Wen-Feng Zhu<sup>1,3</sup> and Dong-Mei Wang <sup>1,3</sup>

<sup>1</sup>The Molecular Medicine Key Laboratory of Liver Injury and Repair, School of Basic Medical Sciences, Henan University of Science and Technology, Luoyang 471003, China

<sup>2</sup>Orthopedic Institute of Henan Province, Luoyang, 471003 Henan, China

<sup>3</sup>Henan Center for Engineering and Technology Research on Prevention and Treatment of Liver Diseases, Luoyang 471003, China

Correspondence should be addressed to San-Qiang Li; [sanqiangli2001@163.com](mailto:sanqiangli2001@163.com), Ping Wang; [glorywangping@163.com](mailto:glorywangping@163.com), and Dong-Mei Wang; [wdmzgadyx@hotmail.com](mailto:wdmzgadyx@hotmail.com)

Received 24 November 2021; Revised 30 April 2022; Accepted 11 May 2022; Published 6 June 2022

Academic Editor: Kazim Husain

Copyright © 2022 Yong-Yong Zhang et al. This is an open access article distributed under the Creative Commons Attribution License, which permits unrestricted use, distribution, and reproduction in any medium, provided the original work is properly cited.

Alcoholic liver injury is a major global public health concern at present. The ADAM9 gene plays a crucial role in the occurrence and development of various liver diseases, but its role in acute alcoholic liver injury remains ambiguous. In this study, a chimeric single-guide RNA targeting the genomic regions of mouse ADAM9 was designed using the clustered regularly interspaced short palindromic repeats (CRISPR)/CRISPR-associated protein 9 (Cas9) technology. Next, the role of ADAM9 in acute alcoholic liver injury *in vitro* in cultured mouse cells and *in vivo* in a hydrodynamic injection-based alcoholic liver injury mouse model was documented. The findings of this study suggest that ADAM9 induces by regulating cell proliferation, apoptosis, and stress metabolism in mice. Thus, inhibiting the expression of ADAM9 gene using CRISPR/Cas9 can attenuate alcohol-induced acute liver injury in mice.

## 1. Introduction

Alcoholic liver disease (ALD) has high rates of morbidity and mortality and has become a severe and challenging health problem worldwide [1]. In western countries, 50%–75% cases of cirrhosis arise because of excessive alcohol consumption, and approximately 15,000–20,000 Americans die annually of ALD. In China, following viral hepatitis, ALD is the second leading cause of liver injury. ALD refers to a series of liver damage caused by long-term or excessive drinking, including hepatic steatosis, steatohepatitis, and fibrosis, which could advance to hepatocellular carcinoma in severe cases [2–4]. Several studies have investigated the mechanism of alcoholic liver injury and have shown that it is closely associated with oxidative stress, apoptosis and proliferation, production of a large amount of reactive oxygen species, and alcohol metabolites [5]. However, the pathogenesis of liver injury

remains unclear. ADAM9, a highly studied a disintegrin and metalloproteinase (ADAM) family member, is involved in the development and molecular mechanisms of various diseases [6]. Previously, ADAM9 was found to regulate hepatocyte proliferation and apoptosis, angiogenesis, and cytochrome P450 family 2 subfamily E member 1 (CYP2E1) expression by activating the interleukin-6 (IL-6) transduction signal and played an important protective role in CCL4-induced acute liver injury in mice [7]. Because ALD is similar to CCL4-induced chemical liver injury, this study was conducted to further explore the role of ADAM9 in the process of alcohol-induced liver injury.

The ADAM family members, also known as metalloprotease-like disintegrin-like cysteine-rich proteins, are type I transmembrane secretory glycoproteins that possess integrin and metalloproteinase functions. The proteins encoded by the ADAM gene usually contain 800–1200

amino acids and sequentially conserved domains [8] named, from the *N*-terminus to the *C*-terminus, as follows: signal domain, prodomain, metalloproteinase domain, disintegrin domain, cysteine-rich domain, epidermal growth factor-like domain, transmembrane domain, and cytoplasmic tail [9]. ADAM proteins are widely expressed in various tissues and play several different roles. They are extensively involved in the inflammatory response, allergies, tumor development and metastasis, and immune diseases [10]. Studies have found that ADAM9 is associated with the occurrence, development, and metastasis of hepatocellular carcinoma [11, 12] and that many liver cancers often develop gradually from ALD [13]. Therefore, the function of ADAM9 during liver injury was studied. Understanding its molecular mechanisms could allow us to detail the liver injury process and provide a theoretical basis to prevent its further development into liver cancer.

## 2. Materials and Methods

**2.1. Cell Culture and Transfection.** Cell culture: mouse C2C12 myoblasts were purified at the Shanghai Fudan University Biomedical Research Institute and maintained in Dulbecco's modified Eagle medium (DMEM) supplemented with 10% fetal bovine serum and 100 IU/mL penicillin (Solarbio, Shanghai, China). Cells were incubated at 5% CO<sub>2</sub> and saturated humidity at 37°C with 100 µg/mL streptomycin. Transfection was performed using Lipofectamine 3000 (Thermo Fisher Scientific, USA).

**2.2. Single-Guide RNA (sgRNA) Design and Plasmid Construction.** To design the sgRNAs targeting the ADAM9 gene sequences (obtained from NCBI), the online tool developed by Prof. Feng Zhang (<http://crispr.mit.edu/>) was used. To disrupt the *Pep\_M12B\_propep* and *ZnMc* domains, the gene on exon 2 and exon 12 (corresponding to residues 44 and 406) needed to be cleaved. Following a comparative analysis, three clustered regularly interspaced short palindromic repeat (CRISPR) sequences were synthesized (Figure 1). In total, three sgRNAs were designed and three 3-in-1 plasmids were synthesized: pYSY-CMV-Cas9-U6-Adam9-sgRNA1-EFla-Puromycin, pYSY-CMV-Cas9-U6-Adam9-sgRNA2-EFla-Puromycin, and pYSY-CMV-Cas9-U6-Adam9-sgRNA3-EFla-Puromycin, where CMV, U6, and EFla were the Cas9, Adam9-sgRNA1, and puromycin gene promoters, respectively. The synthesized plasmids were amplified by polymerase chain reaction (PCR) and verified by electrophoresis. Positive clones were found at approximately 100 bp (Figure 2).

**2.3. Effective Plasmid Screening.** Equal proportions of the three plasmids were mixed and transfected into mouse C2C12 myoblasts using Lipofectamine 3000. When the concentration of transfected cells reached a confluency of approximately 70%, they were treated with puromycin (50 µg/µL) to screen for single-cell cloning. After extensive cell expansion, cellular genomic DNA was extracted using a genomic DNA extraction kit (Aisijin Biotech Ltd., Shenzhen, China) and PCR was performed. The following primer sequences were used: ADAM9-Exon2-Forward: 5'-TGACCT

GGAACTCACAAA-3', ADAM9-Exon2-Reverse: 5'-TCCA CTCCTTCATTCTG-3', ADAM9-Exon11-Forward: 5'-GGTCTGTTGATGCCTGAT-3', ADAM9-Exon11-Reverse 5'-ATGTAATATGCCCTACCC-3'. PCR was performed in 25 µL of a solution containing 1 µL Oligo-F, 1 µL Oligo-R, 1 µL cDNA, 12.5 µL 2× Es Taq MasterMix, and 9.5 µL RNase-free H<sub>2</sub>O (all from Shanghai Shengggong Biotech Ltd.), under the following conditions: 30 cycles at 94°C for 30 s, 52.5°C for 30 s, and 70°C for 30 s, followed by a 10 min extension step at 70°C. After agarose gel electrophoresis, the PCR products were recovered using a gel extraction kit (OMEGA, USA) and sent to Shanghai Shengggong Biotech Ltd. for sequencing.

Finally, only the sgRNA3 sequence was found to differ significantly from the original sequence (Figure 3). The C2C12 cells were transfected with the sgRNA3 plasmid again to confirm its efficiency and the proteins extracted from stably expressing cells for the purpose of immunoblotting. The sgRNA3-transfected cells had considerably lower levels of ADAM9 than normal cells (Figure 4).

**2.4. Animals and Experimental Design.** Male BALB/c mice (6–8 weeks old, 22 ± 2 g) were purchased from the experimental animal center of the Henan province. All animals were allowed to feed on laboratory chow and allowed 1 week to adapt to the environment before the experiments. All the protocols complied with the guidelines of the National Animal Care and Use Committee of China. In addition, all the animals received care in compliance with the Principles of Laboratory Animal Care.

The mice were randomly divided into three groups (10 mice/group): normal group (no treatment), saline+alcohol group (positive control group subjected to a tail vein injection of normal saline and alcoholic gavage), and ADAM9-sgRNA3+alcohol group (experimental group subjected to a tail vein injection of 60 ng/mice of sgRNA3 plasmids followed by alcoholic gavage) [14]. In the positive control and experimental groups, the mice were fed with 56% (*v/v*) alcohol (Red Star Erguotou Liquor, 56°C, Beijing, China) (24 ml/kg) via oral gavage at the end of the third day after the tail vein injection. The mice were starved for 24 h after alcohol gavage and euthanized by cervical dislocation to collect blood and harvest liver tissues.

**2.5. Serum Transaminase Activity Detection.** Blood samples were collected from the eyeballs of all the mice at 24 h after alcohol administration, and the completely coagulated blood (4000 rpm, 5 min) was centrifuged to obtain serum. The serum aspartate aminotransferase (AST) and alanine aminotransferase (ALT) activities were determined using a commercial assay kit (Xinyu Biological Technology Ltd., Shanghai, China) [15]. This kit is based on double antibody sandwich enzyme-linked immunosorbent assay method. The anti-mouse ALT antibody is coated on the micro enzyme-labeled plate to capture ALT from the serum sample. Then, the biotinylated anti-mouse ALT antibody followed by horseradish peroxidase-labeled avidin was added. Biotin specifically interacts with avidin to form an immune complex, and finally, the chromogenic substrate was added. The optical density (OD) was measured at 450 nm using a microplate reader, and ALT concentration

Exon 2  
 ACTTGGAAACAGACTGTCCATCTTTCTTCTTATGAAATTATTACT **GGT** TGGAGATTAACTAGAGAAAG AAGGGGAA  
CTCTG **GGC** CCCAGTTCACAGCAG

Exon 11  
 TTTGGGCAAATCACTGTGGAGACATTTGCAT TCCATTGTGCTCATGAATT **GGC** GCATAACCTTGAATGAATCAT  
 GATGATGGGAGAGAGTGTCTTCTGTGGAGCAAAGAGCTGTATCATGAATTCAGGAGCATC

FIGURE 1: CRISPR sequences of the mouse ADAM9 gene. The underlined portion and yellow highlights indicate the CRISPR sequences, and the red highlight indicates the protospacer adjacent motif (PAM) sequence GG (RC: CCN).

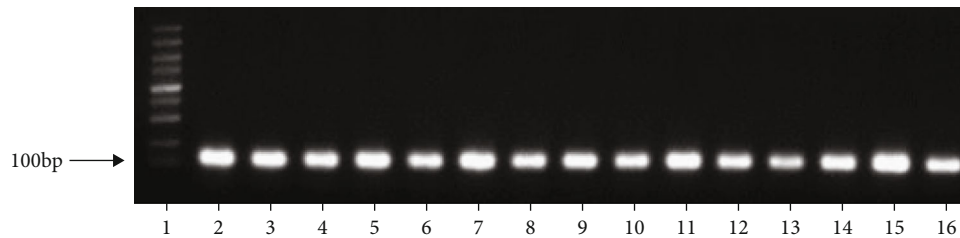


FIGURE 2: Electrophoresis profiles of transformant positive clones obtained by PCR. The band of approximately 100 bp was a positive clone, and the leftmost lane contained the DNA marker: 100, 250, 500, 750, 1000, 1500, 2000, 3000, and 5000 bp. Lanes 2–6: pYSY-CMV-Cas9-U6-ADAM9-gRNA1-EFla-Puromycin clones; lanes 7–11: pYSY-CMV-Cas9-U6-ADAM9-gRNA2-EFla-Puromycin clones; lanes 12–15: pYSY-CMV-Cas9-U6-ADAM9-gRNA3-EFla-Puromycin clones.

Sequence ADAM9 (wild type)	1	GGTCTGTTGATGCTGATTATCG	38
Sequence ADAM9 (sgRNA inhibition)	1	GGTCTGTTGATGCTGATTATCG	15
Sequence ADAM9 (wild type)	39	TGGATTTCTGTCAGCTGCTGCATGTATG	76
Sequence ADAM9 (sgRNA inhibition)	16	CTCTGTTGATGCTGATTATCG	53
Sequence ADAM9 (wild type)	77	GGGACACCTGCTGCTGCTGCTGCTGCTG	113
Sequence ADAM9 (sgRNA inhibition)	54	CTCTGTTGATGCTGATTATCG	82
Sequence ADAM9 (wild type)	114	GGGATTTCTGTCAGCTGCTGCATGTATG	151
Sequence ADAM9 (sgRNA inhibition)	83	CTCTGTTGATGCTGATTATCG	119
Sequence ADAM9 (wild type)	152	GGGACACCTGCTGCTGCTGCTGCTGCTG	189
Sequence ADAM9 (sgRNA inhibition)	120	CTCTGTTGATGCTGATTATCG	157
Sequence ADAM9 (wild type)	190	GGGATTTCTGTCAGCTGCTGCATGTATG	226
Sequence ADAM9 (sgRNA inhibition)	158	CTCTGTTGATGCTGATTATCG	194
Sequence ADAM9 (wild type)	227	GGGACACCTGCTGCTGCTGCTGCTGCTG	264
Sequence ADAM9 (sgRNA inhibition)	195	CTCTGTTGATGCTGATTATCG	232
Sequence ADAM9 (wild type)	265	GGGATTTCTGTCAGCTGCTGCATGTATG	301
Sequence ADAM9 (sgRNA inhibition)	233	CTCTGTTGATGCTGATTATCG	270
Sequence ADAM9 (wild type)	302	TGGATTTCTGTCAGCTGCTGCATGTATG	337
Sequence ADAM9 (sgRNA inhibition)	271	CTCTGTTGATGCTGATTATCG	308
Sequence ADAM9 (wild type)	338	GGGATTTCTGTCAGCTGCTGCATGTATG	375
Sequence ADAM9 (sgRNA inhibition)	309	CTCTGTTGATGCTGATTATCG	344
Sequence ADAM9 (wild type)	376	GGGACACCTGCTGCTGCTGCTGCTGCTG	413
Sequence ADAM9 (sgRNA inhibition)	345	CTCTGTTGATGCTGATTATCG	381
Sequence ADAM9 (wild type)	414	GGGATTTCTGTCAGCTGCTGCATGTATG	451
Sequence ADAM9 (sgRNA inhibition)	382	CTCTGTTGATGCTGATTATCG	419
Sequence ADAM9 (wild type)	452	GGGACACCTGCTGCTGCTGCTGCTGCTG	489
Sequence ADAM9 (sgRNA inhibition)	420	CTCTGTTGATGCTGATTATCG	445
Sequence ADAM9 (wild type)	490	ATTACAT	496
Sequence ADAM9 (sgRNA inhibition)	446		445

FIGURE 3: ADAM9 DNA sequence alignment results. Wild type: the ADAM9 DNA sequence of wild mice. sgRNA inhibition: ADAM9 DNA sequence of mouse C2C12 myoblast transfected with sgRNA 3. Sequencing results compared using the DNAssist software.

in mice was proportional to the OD. The enzyme activity was expressed in international unit per liter (IU/L).

**2.6. Histopathological Examination.** The isolated mouse liver samples were fixed in 10% formaldehyde for 24 h and dehydrated, and tissue wax blocks were then prepared. Sections of 5 μm thickness were cut from each paraffin-embedded tis-

sue and stained with hematoxylin and eosin [16, 17]. Hepatocyte necrosis was photographed using a digital microscope system (Moticam Pro Motic, Xiamen, China), and the hepatocyte necrosis rate was scored using the following scale: no lesion = 0, <2 lesions/visual field = 1, 2 – 4 lesions/visual field = 2, and >4 lesions/visual field = 3.

**2.7. Hoechst 33258 Staining Assay for Hepatocyte Apoptosis.** Apoptosis in the hepatocytes of the different groups of mice was analyzed using a commercial kit (BEYOTIME, Shanghai, China) [18]. The stained sections were assessed microscopically, and photographs were taken using a digital image capture system (Olympus). A microscope was used for counting normal and apoptotic cells. The apoptotic rate was calculated as follows: apoptotic rate = [number of apoptotic cells/total number of cells] × 100%. This experiment was repeated thrice.

**2.8. Periodic Acid-Schiff (PAS) Staining.** After conventional gradient dewaxing and hydration, the tissue sections were incubated in 0.8% periodic acid for 15 min, then stained with Schiff reagent for 20 min, and finally counterstained with hematoxylin [19]. Using an optical microscope, 10 representative fields of each group were randomly selected for observation, and their optical density was analyzed using the Motic Images Advanced 3.2 software (Moticam Pro Motic, Xiamen, China). This experiment was repeated three times.

**2.9. Western Blotting.** Proteins were quantified using a BCA Protein Assay Kit (Solarbio, Shanghai, China), and 50 μg of the sample was subjected to sodium dodecyl sulfate-polyacrylamide gel electrophoresis; the proteins were then electrotransferred onto a nitrocellulose membrane. Next,

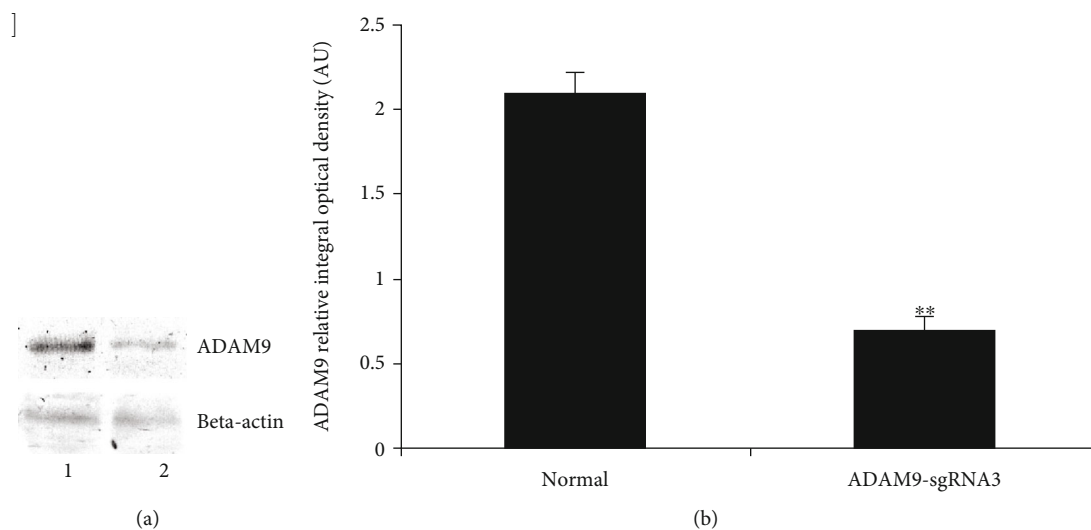


FIGURE 4: ADAM9 protein expression in mouse C2C12 myoblasts transfected with ADAM9-sgRNA3. (a) Detection of ADAM9 protein expression in normal C2C12 cells and C2C12 cells transfected with sgRNA3 by western blotting. (b) ADAM9 expression levels were quantified using Gel-Pro Analyzer 4.0 software (Media Cybernetics Inc.). Band intensities were normalized to  $\beta$ -actin. AU = arbitrary unit. \*\* $P < 0.01$ : significant differences between normal C2C12 cells and C2C12 cells transfected with sgRNA3.

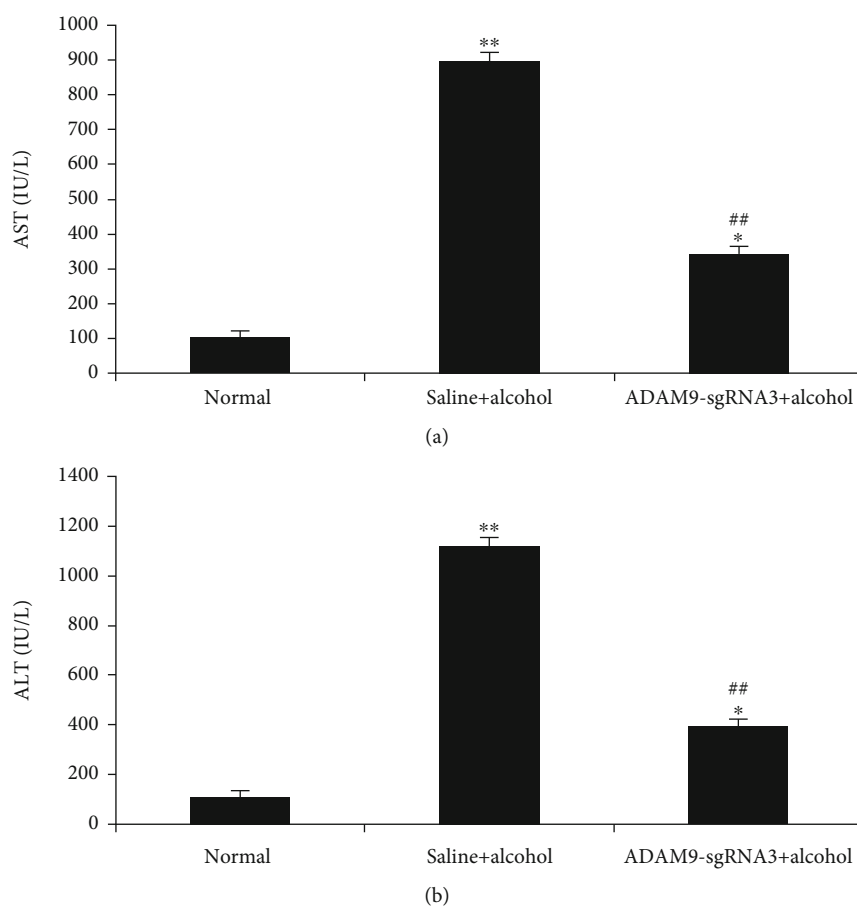


FIGURE 5: Serum (a) AST and (b) ALT levels in the mice 24 h after alcohol treatment. \*\* $P < 0.01$  and \* $P < 0.05$ : significant differences between the positive control or experimental group and the negative control group. ## $P < 0.01$ : significant difference between the experimental and positive control groups. Every experiment was repeated three times.

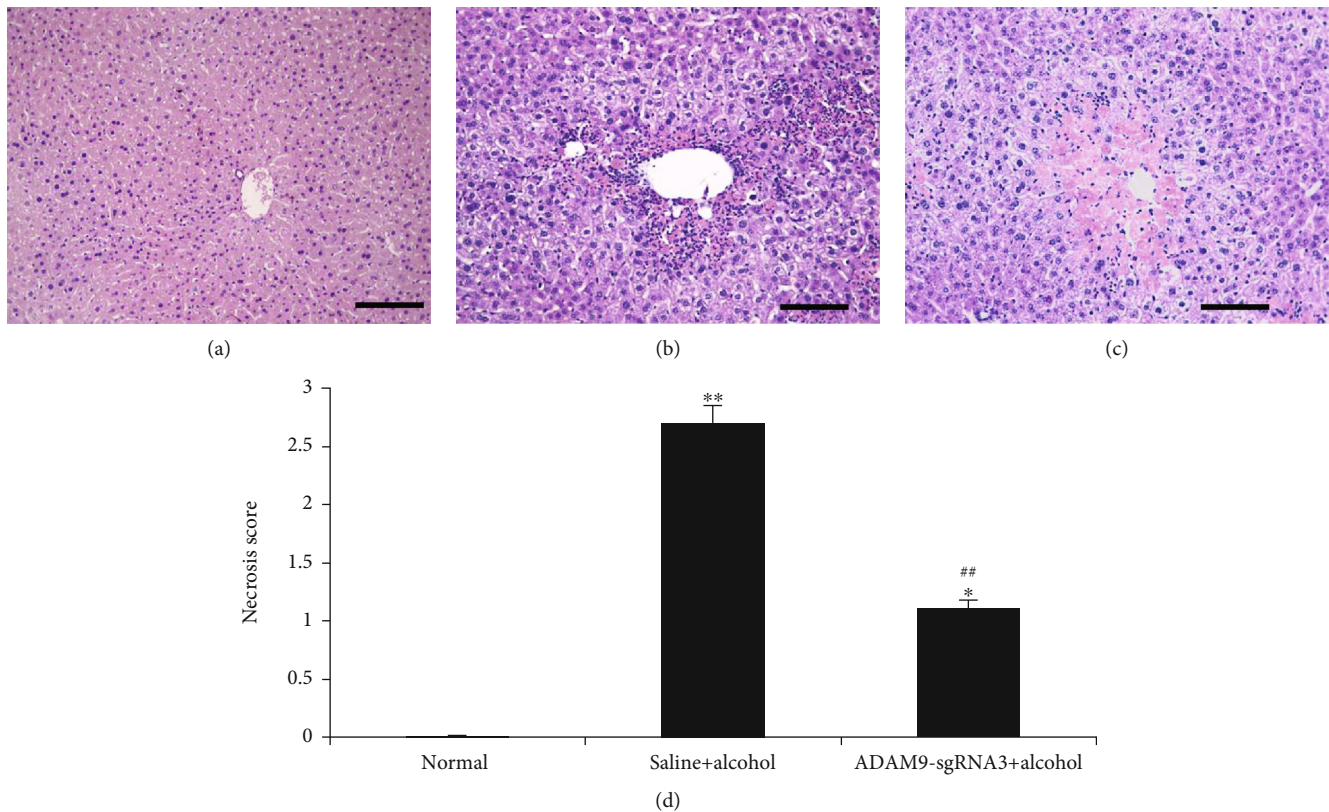


FIGURE 6: Histologic examination of liver injuries in the mice 24 h after alcohol treatment. HE staining in the (a) negative control group, (b) positive control group, and (c) experimental group. (d) Necrotic score. \*\* $P < 0.01$  and \* $P < 0.05$ : significant differences between the positive control or experimental group and the negative control group. ## $P < 0.01$ : significant difference between the experimental and positive control groups. Every experiment was repeated three times (scale bar: 50  $\mu\text{m}$ ).

the membrane was treated with monoclonal antibodies against mouse ADAM9, heat shock protein 27 (HSP27), heat shock protein 70 (HSP70), proliferating cell nuclear antigen (PCNA), B cell lymphoma protein 2 (Bcl-2), Bcl-2-associated X (Bax), caspase-3, vascular endothelial growth factor (VEGF), and phosphorylated signal transducer and activator of transcription 3 (p-STAT3) (Santa Cruz). The signal was detected by employing a horseradish peroxidase detection system using diaminobenzidine (Sigma). The protein bands were quantified with the Gel-Pro Analyzer software 4.0 (Media Cybernetics Inc., Bethesda, MD) and their intensities normalized to beta-actin. Every experiment was repeated thrice [7].

**2.10. In Vitro Experiments.** The L02 hepatocytes obtained from Shanghai Fudan University Biomedical Research Institute were purified and cultured under 5%  $\text{CO}_2$  at 37°C in modified DMEM supplemented with 15% fetal bovine serum, 100 units/mL penicillin, and 100 units/mL streptomycin. When the cells on the 10  $\text{cm}^2$  dish reached a confluency of 70%, they were separated into four groups: normal (nontransfected, untreated), normal+ADAM9-sgRNA3 (plasmid-transfected, untreated), saline+alcohol (nontransfected, alcohol-treated), and ADAM9-sgRNA+alcohol (plasmid-transfected, alcohol-treated) groups. The L02 hepatocytes were transfected with the screened sgRNA3

plasmid (plasmid-transfected cells), and the monoclonal cell line deficient in ADAM9 gene was screened and cultured using the aforementioned monoclonal cell screening method. When cells reached 70% confluency, they were treated with alcohol (30  $\mu\text{L}/\text{mL}$ ) for 24 h (alcohol-treated cells).

**2.11. Statistical Analysis.** All the data were expressed as the mean  $\pm$  SEM. Comparisons between two groups were conducted using the independent sample *t*-test, and the one-way analysis of variance (ANOVA) test was used for comparisons between more than two groups. *P* values of  $<0.05$  and  $<0.01$  were considered statistically significant and highly significant, respectively. All statistical calculations were performed using the SPSS 19.0 software (SPSS, Inc., Chicago, IL, USA).

### 3. Results

**3.1. Serum ALT and AST Enzyme Activities in Mice.** Figure 5 shows that the positive control and experimental groups (both of which received ethanol treatment) had significantly higher serum AST and ALT levels than the normal group ( $P < 0.05$  and  $P < 0.01$ ). Moreover, the experimental group had significantly lower serum AST and ALT levels than the positive control group ( $P < 0.01$ ).

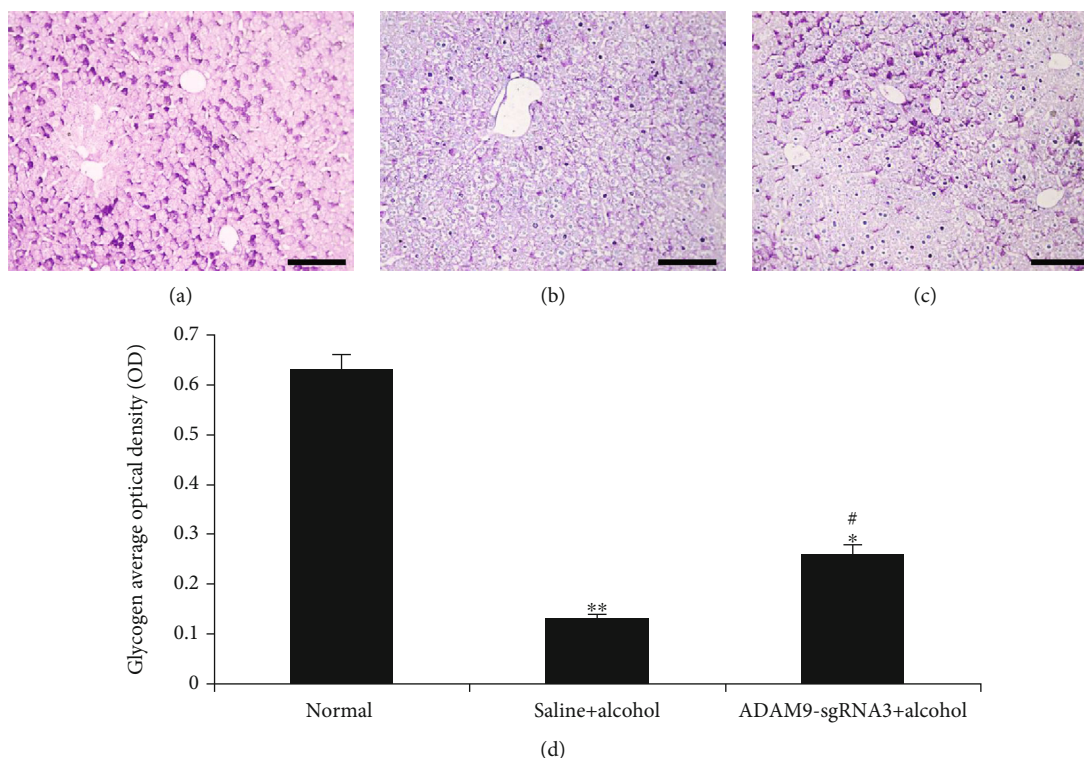


FIGURE 7: Glycogen quantification in liver sections prepared from mice 24 h after alcohol treatment. PAS staining in the (a) negative control group, (b) positive control group, and (c) experimental group. (d) Staining quantification using the Motic Images Advanced 3.2 software (Motic China Group Co., Ltd., Xiamen, China). \*\* $P < 0.01$  and \* $P < 0.05$ : significant differences between the positive control or experimental group and the negative control group. # $P < 0.01$ : significant difference between the experimental and positive control groups. Every experiment was repeated three times (scale bar: 50  $\mu\text{m}$ ).

**3.2. HE Staining for the Detection of Hepatocyte Necrosis Rate.** Figure 6 shows that the positive control and experimental groups showed the presence of liver injuries that the normal group did not ( $P < 0.05$  or  $P < 0.01$ ). Besides, the experimental group had a significantly lower hepatocyte necrosis score than the positive control group ( $P < 0.01$ ).

**3.3. PAS Staining for Hepatic Glycogen Detection.** The experimental and positive control groups showed significantly higher hepatic glycogen consumption than the negative control group ( $P < 0.05$  and  $P < 0.01$ ; Figure 7). However, hepatic glycogen consumption was lower in the experimental group than in the positive control group ( $P < 0.05$ ; Figure 7).

**3.4. Hoechst 33258 Staining for Hepatocyte Apoptosis Detection.** Figure 8 shows that ethanol treatment markedly increased the hepatocyte apoptosis rate (experimental and positive control groups vs. negative control group:  $P < 0.05$  and  $P < 0.01$ , respectively). However, the hepatocyte apoptosis rate was lower in the experimental group than in the positive control group ( $P < 0.05$ ).

**3.5. Western Blotting Results of the Experiment on Mice.** Figure 9 shows that ADAM9 expression was higher in the positive control and experimental groups than in the negative control group ( $P < 0.05$  and  $P < 0.01$ ). Besides, ADAM9

expression was significantly lower in the experimental group than in the positive control group ( $P < 0.05$ ). Thus, injecting the plasmid into the tail vein was found to considerably inhibit the expression of ADAM9 gene in the mouse liver tissue. Meanwhile, the positive control and experimental groups had significantly higher expression levels of HSP27, HSP70, Bax, caspase-3, and p-STAT3 than the negative control group and lower expression levels of PCNA, Bcl-2, and VEGF. In addition, the experimental group had higher expression levels of HSP27, HSP70, PCNA, Bcl-2, VEGF, and p-STAT3 than the positive control group and lower expression levels of Bax and caspase-3 (Figure 9).

**3.6. Western Blotting Results of L02 Hepatocytes.** Figure 10 shows a significant increase in the expression of ADAM9 in alcohol-treated stem L02 cells, whereas the expression of the ADAM9 protein was significantly inhibited when the cells were transfected with sgRNA3 plasmid ( $P < 0.05$  and  $P < 0.01$ ). The positive control group had significantly higher expression levels of HSP27, HSP70, Bax, caspase-3, and p-STAT3 and lower expression levels of PCNA, Bcl-2, and VEGF than the negative control group ( $P < 0.05$  and  $P < 0.01$ ). In the experimental group, the expression levels of HSP27, HSP70, Bax, caspase-3, and p-STAT3 were significantly increased, whereas the expression levels of PCNA, Bcl-2, and VEGF were decreased ( $P < 0.05$  and  $P < 0.01$ ), which is similar to that observed in the positive CRISPR

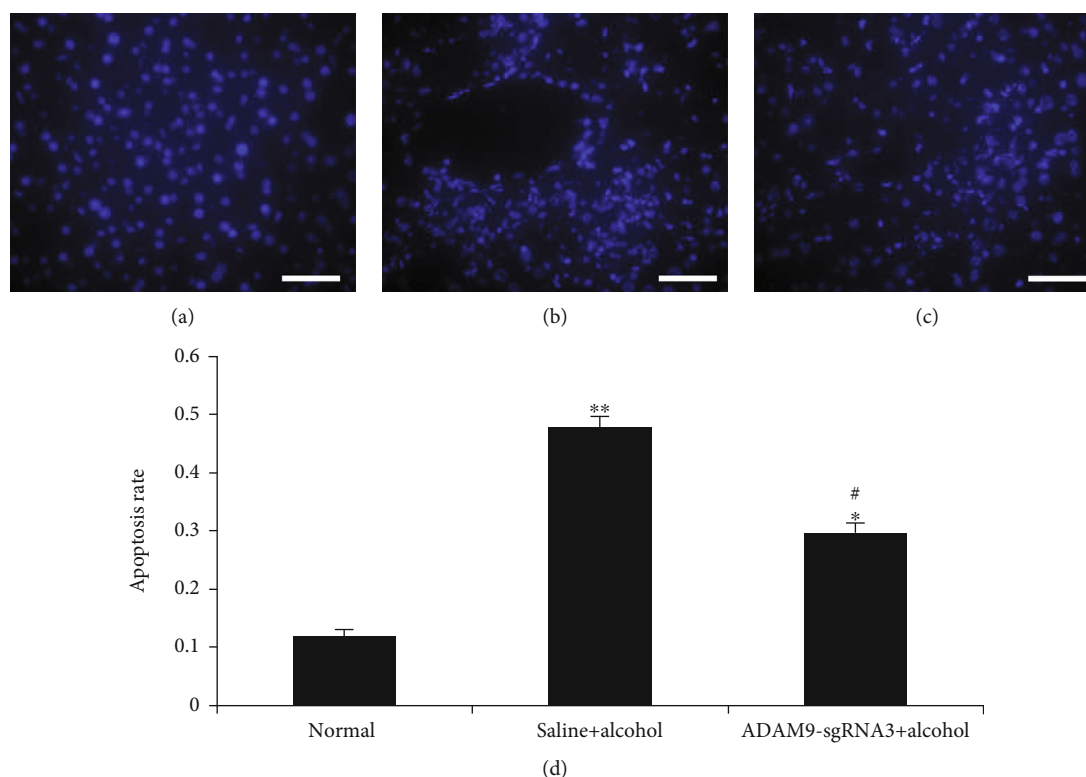


FIGURE 8: Apoptosis analysis of liver sections from mice 24 h after alcohol treatment. Hoechst 33258 staining in the (a) negative control group, (b) positive control group, and (c) experimental group. (d) Apoptotic rate. \*\* $P < 0.01$  and \* $P < 0.05$ : significant differences between the positive control or experimental group and the negative control group. # $P < 0.01$ : significant difference between the experimental and positive control groups. Every experiment was repeated three times (scale bar: 50  $\mu\text{m}$ ).

control group. When the two groups in which ADAM9 gene knockout was performed were compared with the two groups with the ADAM9 gene, i.e., when the normal+sgRNA3 group was compared with the negative control group and the experimental group was compared with the positive control group, the expressions of the HSP27, HSP70, PCNA, Bcl-2, VEGF, and p-STAT3 proteins were significantly increased, whereas only the expressions of Bax and caspase-3 were significantly decreased ( $P < 0.05$  and  $P < 0.01$ ).

#### 4. Discussion

CRISPR/Cas9 is a recently developed genome editing technology that uses sgRNA and the Cas9 nuclease for identifying and editing specific DNA sites; it provides a novel platform for human gene editing. However, because it frequently affects off-target DNA, three sgRNAs were designed and the most successful sgRNA was selected [20, 21] (Figures 1 and 2). sgRNA3 successfully inhibited the expression of ADAM9 gene in the mouse liver (Figure 3). Mouse C2C12 cells were transfected with the three successfully constructed plasmids, screened using puromycin, and the cell DNA extracted for sequencing after the formation of a stable clone. On comparing this sequence with the original sequence, the sgRNA3 plasmid was found to knock out the ADAM9 gene (Figure 3). Next, the cellular protein was extracted and the validity of the sgRNA3 plasmid was veri-

fied again at the protein level (Figures 4, 9(a), 9(b), 10(a), and 10(b)).

The effect of the inhibition of ADAM9 gene expression was initially observed on alcohol-induced acute liver injury. AST and ALT are both tissue enzymes that catalyze the exchange of amino and keto groups between alpha amino and keto acids. Tissue toxicity causes the release of these enzymes into the general circulation, thereby increasing the levels of these enzymes [22]. The results showed that the experimental group had significantly lower serum AST and ALT levels ( $P < 0.05$ , Figure 5) and hepatocyte necrosis score ( $P < 0.05$ , Figure 6) than the positive control group. However, the liver glycogen level in the experimental group was significantly higher than that in the positive control group. Glycogen synthesis in the liver is the main form of energy storage in animals. Liver glycogen content decreased proportionally with increase in the severity of alcoholic liver disease in the early stage [23, 24]. The results of this study showed that alcohol-induced injury decreased the hepatic glycogen content in mice; however, the inhibition of ADAM9 gene expression partially prevented this decrease. These results indicate that ADAM9-sgRNA3 significantly attenuated the severity of alcohol-induced liver injury and suggest that ADAM9 contributes to alcohol-induced liver injury promotion.

The findings of this study showed that after inhibiting the expression of the ADAM9 gene in alcohol-induced acute

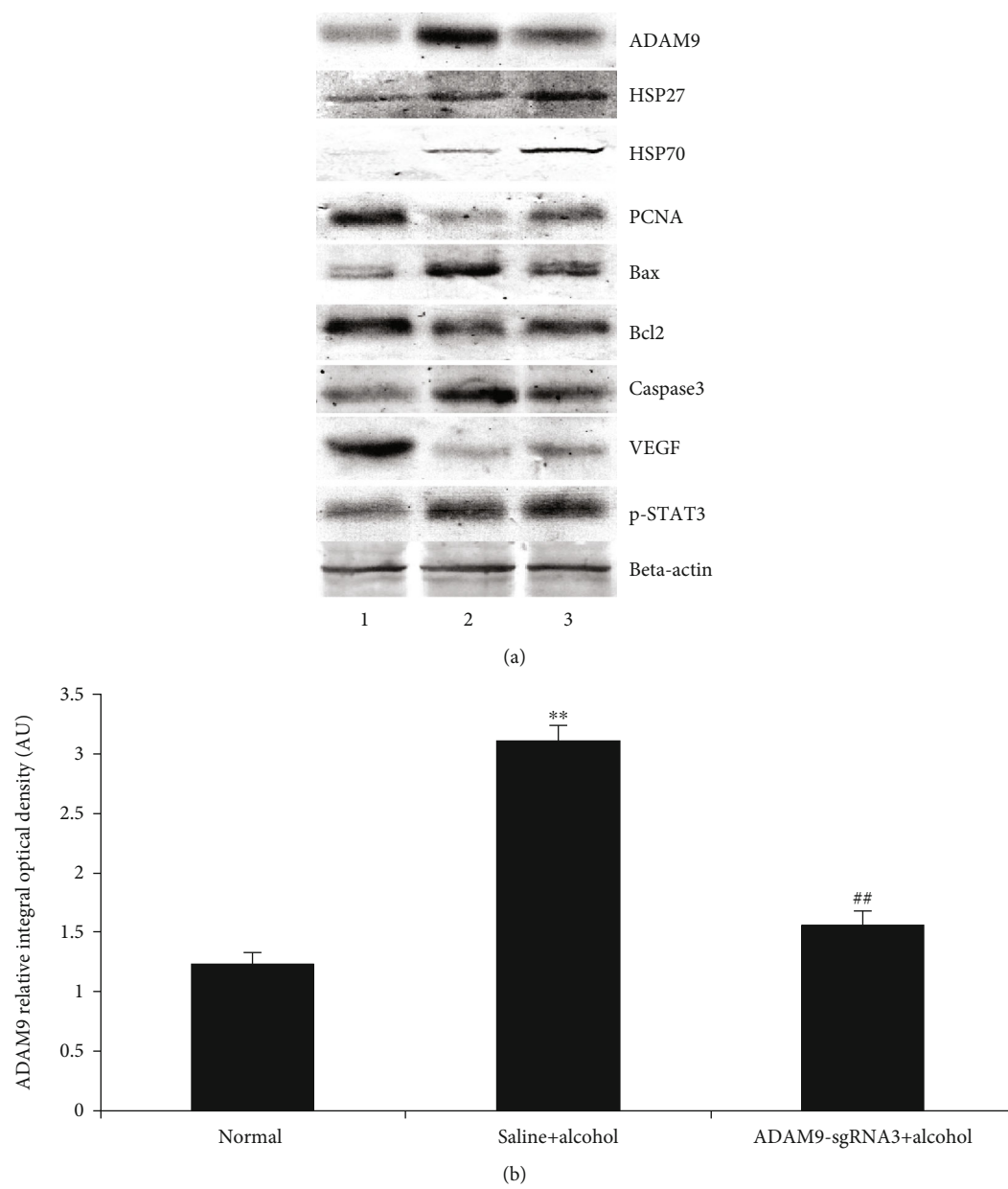
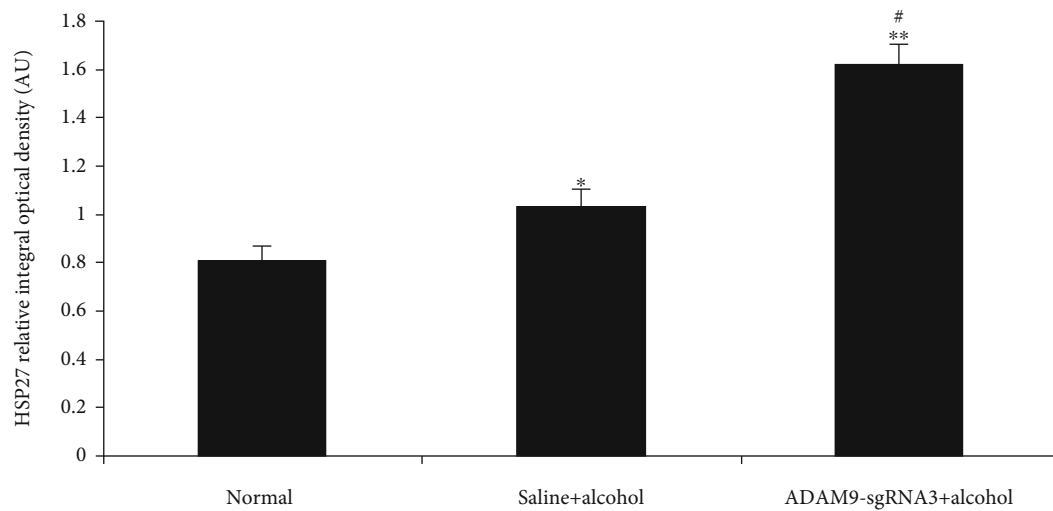
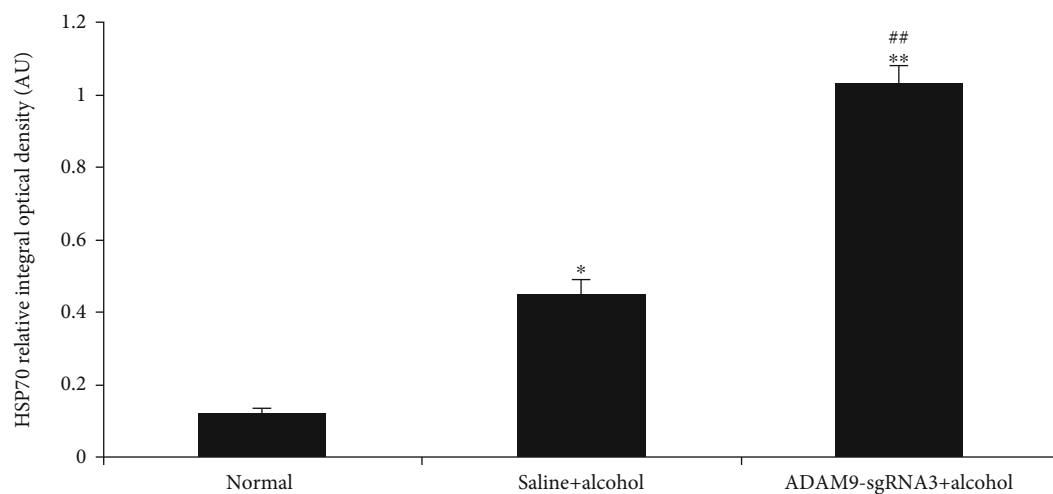


FIGURE 9: Continued.

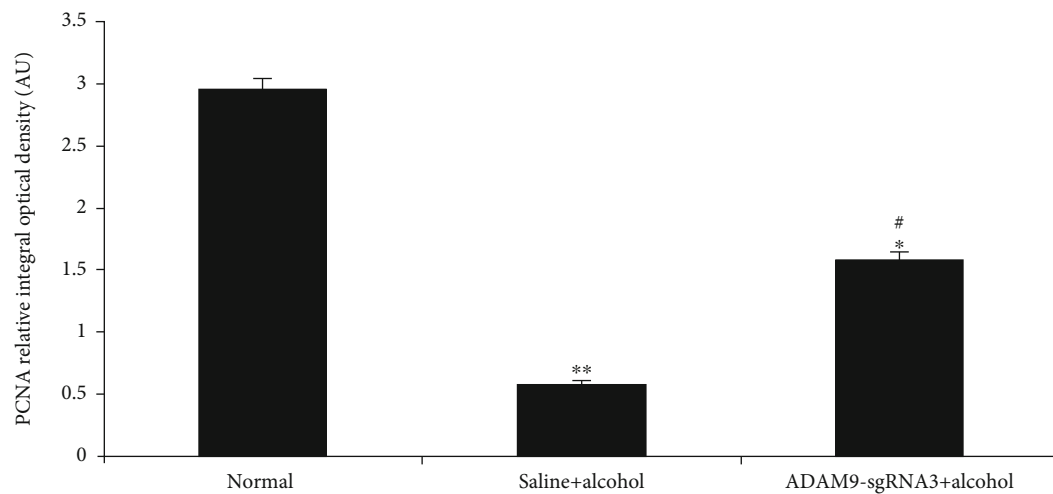




(c)



(d)



(e)

FIGURE 9: Continued.

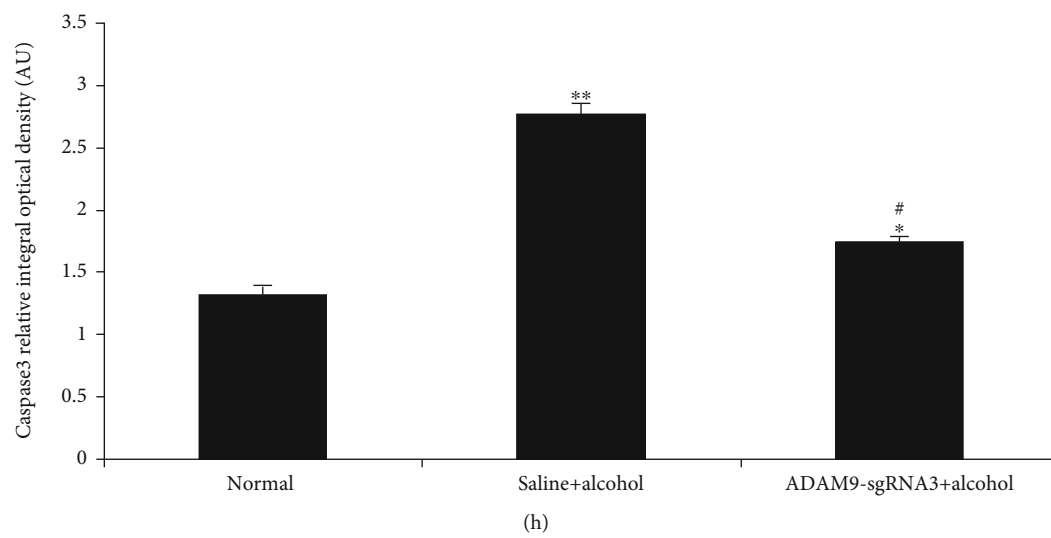
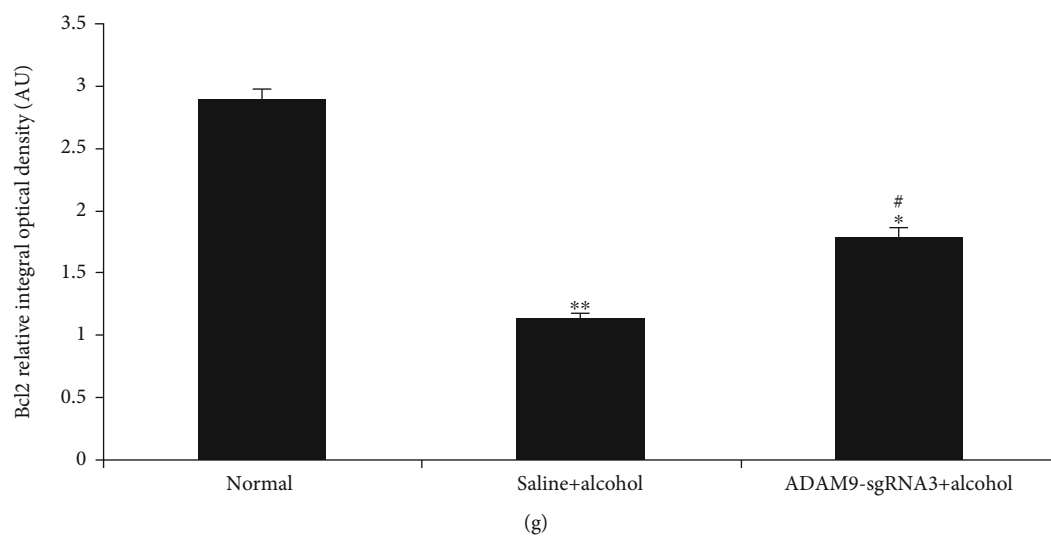
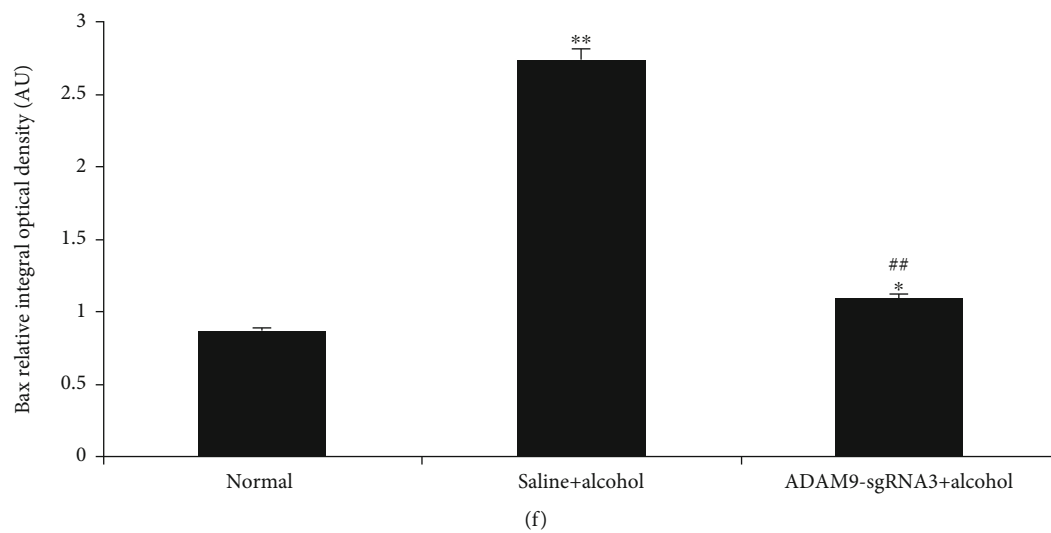


FIGURE 9: Continued.

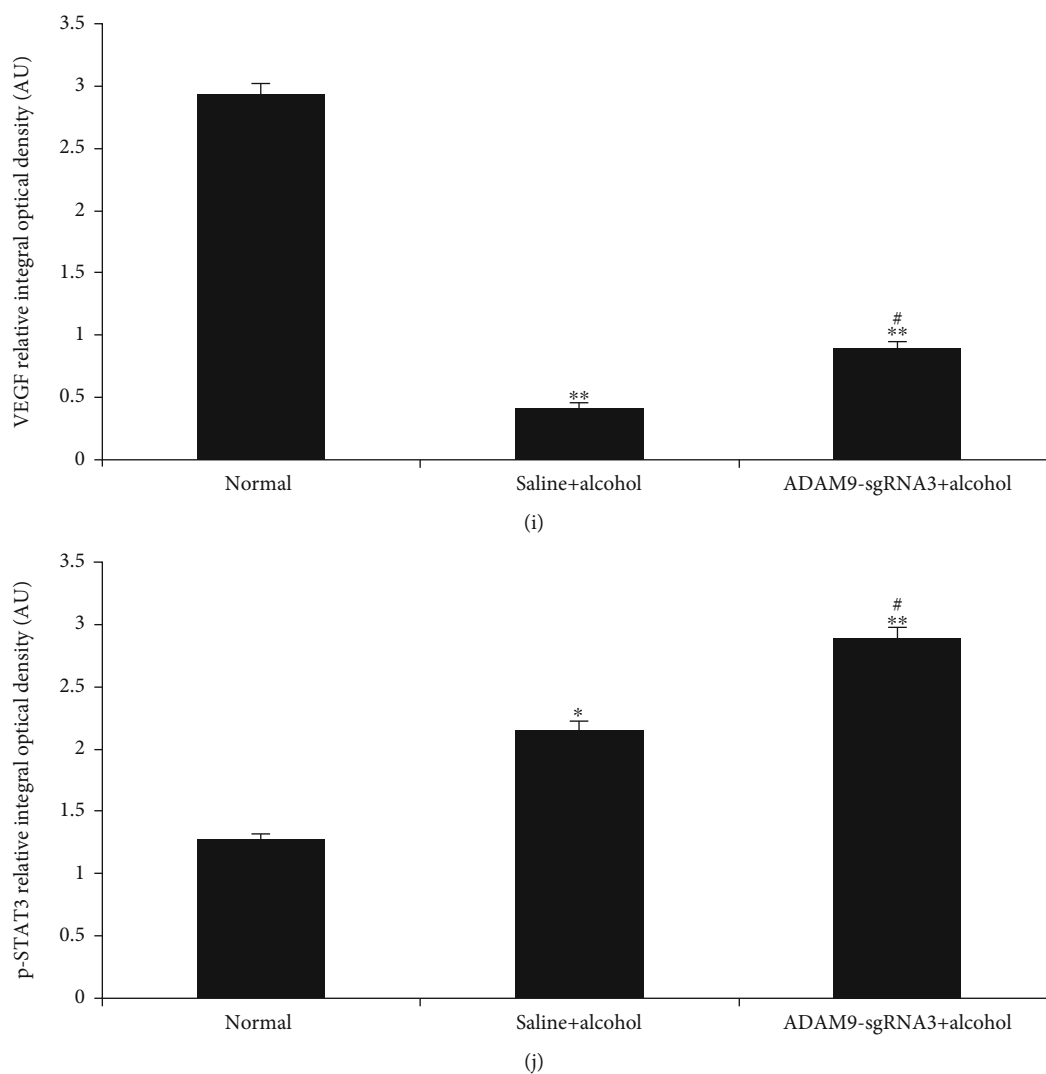
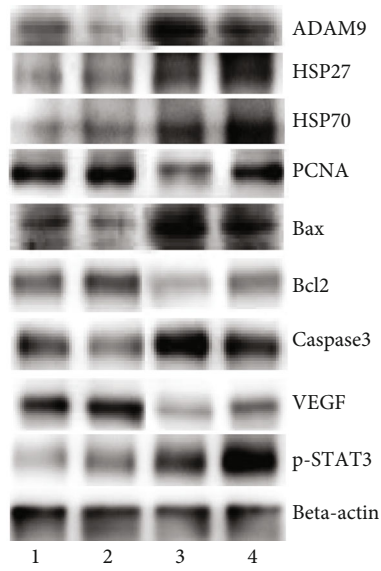


FIGURE 9: The influence of alcohol on the expression of ADAM9, HSP27, HSP70, PCNA, Bax, Bcl-2, caspase-3, VEGF, and p-STAT3 in the liver of mice 24 h after alcohol treatment. (a) Western blotting results. The expression levels of (b) ADAM9, (c) HSP27, (d) HSP70, (e) PCNA, (f) Bax, (g) Bcl-2, (h) caspase-3, (i) VEGF, and (j) p-STAT3 quantified with the Gel-Pro Analyzer 4.0 software (Media Cybernetics Inc.). Band intensities normalized to  $\beta$ -actin. AU = arbitrary unit. \*\* $P < 0.01$  and \* $P < 0.05$ : significant differences between the positive control or experimental group and the negative control group. ## $P < 0.01$  and # $P < 0.05$ : significant differences between the experimental and positive control groups.

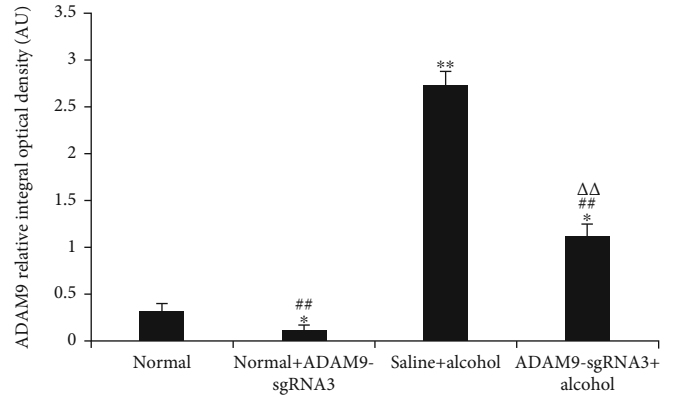
liver injury, the expression of HSP27 and HSP70 further increased in comparison with the positive control group ( $P < 0.05$  and  $P < 0.01$ ) (Figures 9(a), 9(c), 9(d), 10(a), 10(c), and 10(d)). HSP27 and HSP70 are molecular chaperones that are essential for accurate three-dimensional folding of nascent polypeptide chains and proteins and the repair process after protein damage [25]. These molecular chaperones protect proteins and maintain normal cellular physiological activity when external factors promote their mass production. The results of this study showed that silencing the ADAM9 gene increased the expression of HSP27 and HSP70 in the liver of mice. Therefore, ADAM9 may promote liver damage during acute alcoholic liver injury by reducing the expression of heat shock proteins.

The results of this study showed that silencing ADAM9 significantly reduced the apoptosis rate (experimental group

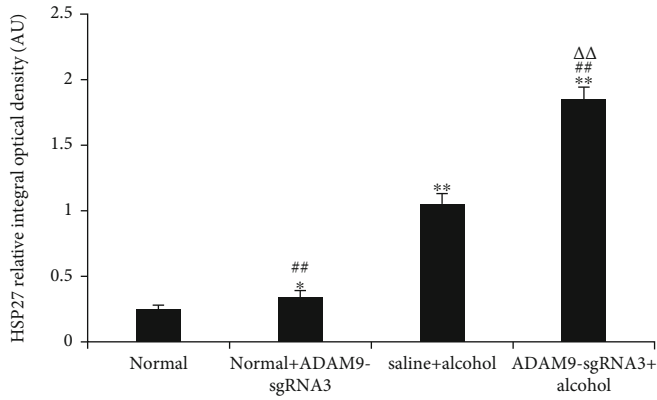
vs. positive control group,  $P < 0.05$ ) (Figure 8). Casp3, Bax, and Bcl-2 are important factors associated with apoptosis. Inhibition of the expression of the ADAM9 gene was shown to significantly reduce the Bax and caspase-3 expression levels and increase those of Bcl-2 ( $P < 0.05$  and  $P < 0.01$ ) (Figures 9(a), 9(f), 9(g), 9(h), 10(a), 10(f), 10(g), and 10(h)). Caspase-3 is a member of the interleukin-1 beta-converting enzyme or cell death effector-3 family, which plays an irreplaceable role in apoptosis, and caspase-3 is the most important terminal cleavage enzyme in the process of apoptosis [26]. Insect Sf9 cells were transfected with caspase-3 gene to induce apoptosis, and this process could be blocked by Bcl-2. Bax and Bcl-2 are important proapoptotic and antiapoptotic markers, respectively, which contribute significantly to the regulation of apoptosis [27, 28]. Therefore, inhibiting the expression of the ADAM9 gene



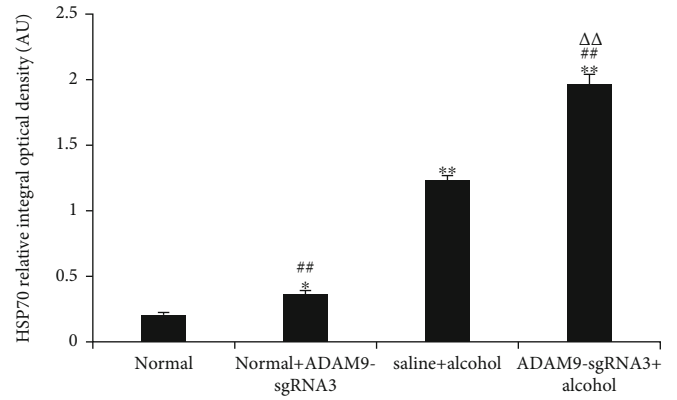
(a)



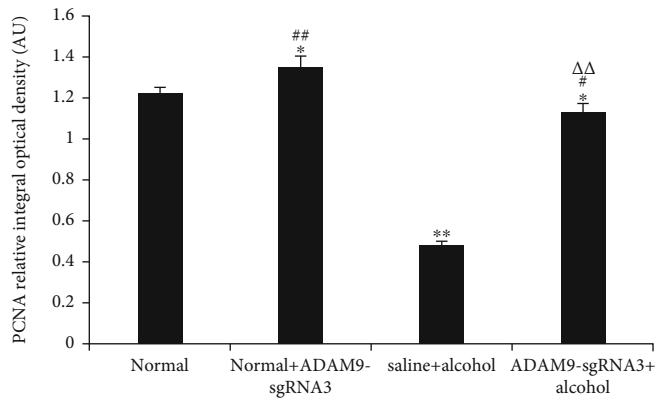
(b)



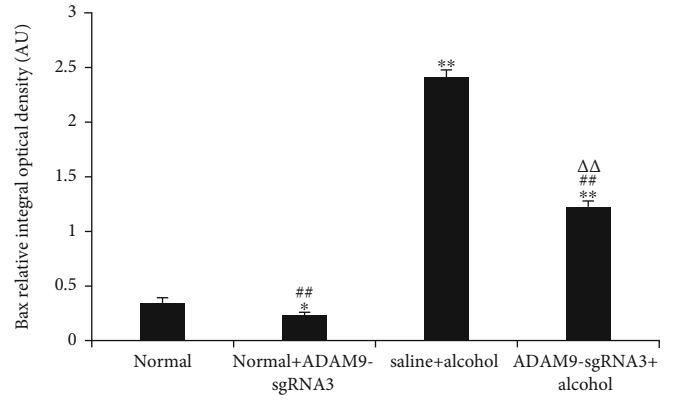
(c)



(d)



(e)



(f)

FIGURE 10: Continued.

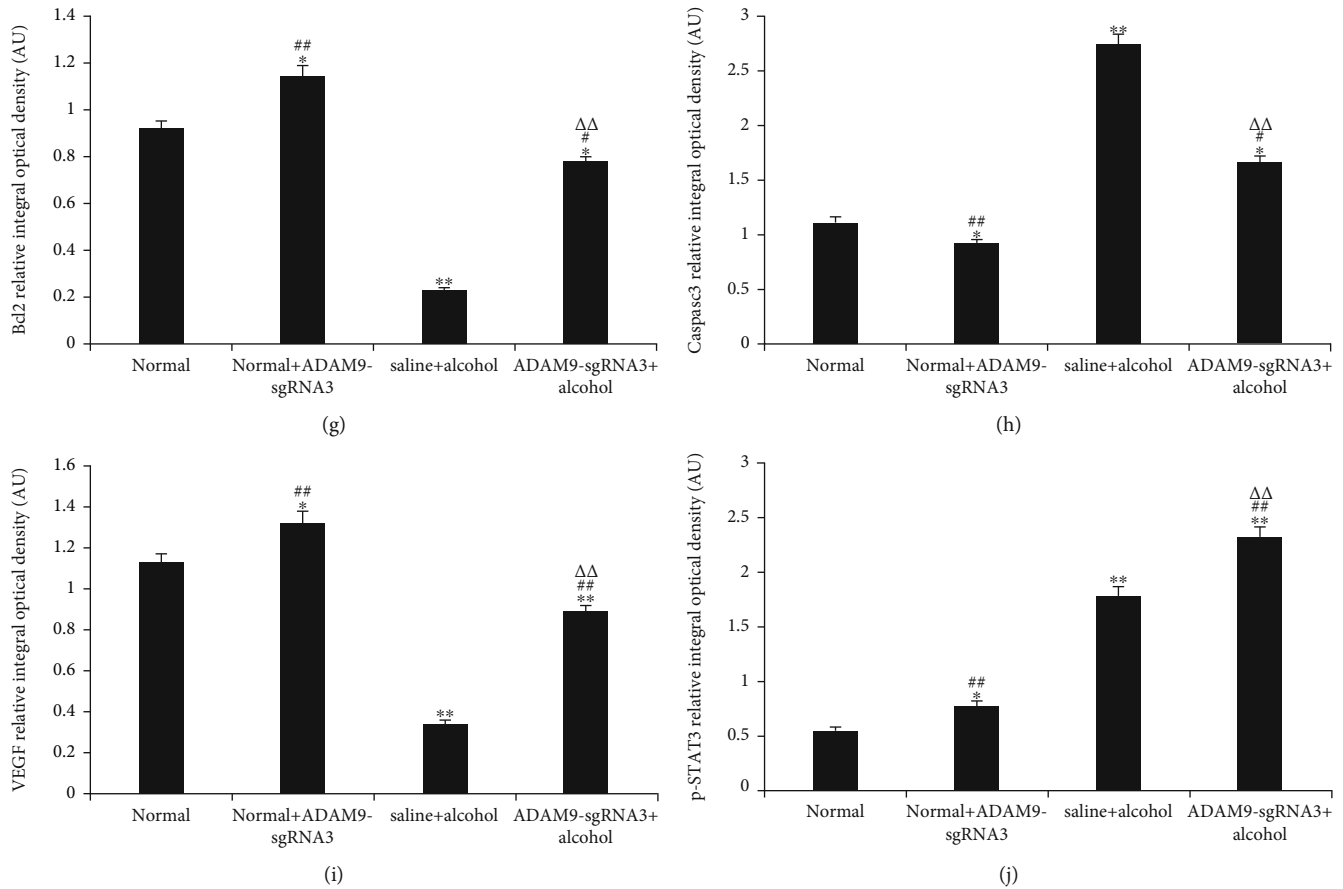


FIGURE 10: In vitro analysis of the effects of alcohol on the expression levels of ADAM9, HSP27, HSP70, PCNA, Bax, Bcl-2, caspase-3, VEGF, and p-STAT3 in hepatic L02 cells. (a) Western blotting results. The expression levels of (b) ADAM9, (c) HSP27, (d) HSP70, (e) PCNA, (f) Bax, (g) Bcl-2, (h) caspase-3, (i) VEGF, and (j) p-STAT3 quantified using Gel-Pro Analyzer 4.0 software (Media Cybernetics Inc.). Band intensities normalized to  $\beta$ -actin. AU = arbitrary unit. \*\* $P < 0.01$  and \* $P < 0.05$ : significant differences between the normal +ADAM9-sgRNA3, saline+alcohol, ADAM9-sgRNA+alcohol, and normal group. ## $P < 0.01$  and # $P < 0.05$ : significant differences between the normal+ADAM9-sgRNA3, ADAM9-sgRNA+alcohol, and saline+alcohol groups.  $\Delta\Delta P < 0.01$  and  $\Delta P < 0.05$ : significant difference between the ADAM9-sgRNA+alcohol group and the normal+ADAM9-sgRNA3 group.

can inhibit apoptosis by upregulating antiapoptotic inhibitors and downregulating proapoptotic factors.

The results of this study showed that ADAM9 knockout significantly upregulated the expression of PCNA in alcohol-induced acute liver injury in mice ( $P < 0.05$  and  $P < 0.01$ ) (Figures 9(a), 9(e), 10(a), and 10(e)). PCNA, synthesized in the nucleus of mammalian cells, plays a crucial role in the cell proliferation cycle. Its expression levels are lower in the G2 to M phase and peak in the S phase, making it a good indicator of the proliferative capacity of cells [29]. It was further demonstrated that the knockout of the ADAM9 gene could promote hepatocyte proliferation in alcohol-induced acute liver injury; i.e., the knockout of the ADAM9 gene can alleviate alcohol-induced acute liver injury.

The findings of this study also showed that inhibition of the ADAM9 gene can significantly promote the expression of VEGF in alcohol-induced acute liver injury ( $P < 0.05$  and  $P < 0.01$ ) (Figures 9(a), 9(i), 10(a), and 10(i)). VEGF is a major cytokine that has multiple functions such as promoting neovascularization, increasing vascular permeability, promoting endothelial cell proliferation, and inhibiting apo-

ptosis. In patients with chronic hepatitis, the expression of VEGF is more pronounced in hepatocytes and sinus spaces in hepatic vascular inflammation, destruction, and obstruction, and its expression in liver tissue increases with the aggravation of liver tissue degeneration and necrosis [30]. The findings of this study suggested that inhibiting the expression of ADAM9 gene significantly increased the expression of VEGF (experimental group vs. positive control group,  $P < 0.05$ ), indicating that ADAM9 promotes liver injury by inhibiting the expression of VEGF during alcoholic liver injury.

The experimental group had significantly higher phosphorylated signal transducer and activator of transcription 3 (p-STAT-3) protein expression levels than the positive control group in alcohol-induced acute liver injury ( $P < 0.05$  and  $P < 0.01$ ) (Figures 9(a), 9(j), 10(a), and 10(j)). p-STAT-3 is a hallmark of the IL-6 signaling pathway activation. Alcohol-stimulated hepatocytes produce multiple factors that activate the IL-6 pathway, including p-STAT3. In the nucleus, activated STAT stimulates the expression of various genes, effectively alleviating inflammatory and

cellular damage during alcoholic liver injury [31]. Thus, inhibiting the expression of ADAM9 enhanced the activation of the IL-6 signaling pathway during acute alcoholic liver injury. Therefore, ADAM9 promotes liver injury by reducing the activation of the IL-6 signaling pathway during acute alcoholic liver injury.

## 5. Conclusion

This study is the first to elucidate the role of ADAM9 in acute alcoholic liver injury and its related molecular mechanisms. ADAM9 promotes liver damage by regulating the expression of genes associated with cell proliferation, apoptosis, stress, and metabolism during acute alcoholic liver injury in mice. Inhibiting the expression of ADAM9 gene using CRISPR/Cas9 technology successfully attenuated alcohol-induced acute liver injury in mice.

## Data Availability

If other people apply, data will be available for them.

## Conflicts of Interest

The authors declare that they have no conflicts of interest.

## Acknowledgments

This work was supported by the Central Plains Science and Technology Innovation Leader Project (No. 214200510004), National Natural Science Foundation of China (82170606), and Luoyang City Science and Technology Plan Project (2101028A). The authors thank all the members of the laboratory where this work was conducted. The experiments comply with the current laws of China.

## References

- [1] W. M. Lee and E. Seremba, "Etiologies of acute liver failure," *Current Opinion in Critical Care*, vol. 14, no. 2, pp. 198–201, 2008.
- [2] B. Gao and R. Bataller, "Alcoholic liver disease: pathogenesis and new therapeutic targets," *Gastroenterology*, vol. 141, no. 5, pp. 1572–1585, 2011.
- [3] J. Liu, Q. Ma, M. Zhang et al., "Alterations of TP53 are associated with a poor outcome for patients with hepatocellular carcinoma: evidence from a systematic review and meta-analysis," *European Journal of Cancer*, vol. 48, no. 15, pp. 2328–2338, 2012.
- [4] A. Miranda-Mendez, A. Lugo-Baruqui, and J. Armendariz-Borunda, "Molecular basis and current treatment for alcoholic liver disease," *International Journal of Environmental Research and Public Health*, vol. 7, no. 5, pp. 1872–1888, 2010.
- [5] Y.-Y. Zhang, S.-Q. Li, Y. Song et al., "The therapeutic effect of Chaihu-Shugan-San in fatty liver disease: a meta-analysis randomized controlled trials," *International Journal of Clinical and Experimental Medicine*, vol. 11, pp. 12880–12888, 2018.
- [6] A. Mazzocca, R. Coppari, R. De Franco et al., "A secreted form of ADAM9 promotes carcinoma invasion through tumor-stromal interactions," *Cancer Research*, vol. 65, no. 11, pp. 4728–4738, 2005.
- [7] S. Q. Li, D. M. Wang, S. Zhu et al., "The important role of ADAM8 in the progression of hepatocellular carcinoma induced by diethylnitrosamine in mice," *Human & Experimental Toxicology*, vol. 34, no. 11, pp. 1053–1072, 2015.
- [8] M. J. Duffy, E. McKiernan, N. O'Donovan, and P. M. McGowan, "Role of ADAMs in cancer formation and progression," *Clinical Cancer Research*, vol. 15, no. 4, pp. 1140–1144, 2009.
- [9] D. F. Seals and S. A. Courtneidge, "The ADAMs family of metalloproteases: multidomain proteins with multiple functions," *Genes & Development*, vol. 17, no. 1, pp. 7–30, 2003.
- [10] R. A. Black and J. M. White, "ADAMs: focus on the protease domain," *Current Opinion in Cell Biology*, vol. 10, no. 5, pp. 654–659, 1998.
- [11] L. Y. Xiang, H. H. Ou, X. C. Liu et al., "Loss of tumor suppressor miR-126 contributes to the development of hepatitis B virus-related hepatocellular carcinoma metastasis through the upregulation of ADAM9," *Tumour Biology*, vol. 39, no. 6, p. 101042831770912, 2017.
- [12] Y. Dong, Z. Wu, M. He et al., "ADAM9 mediates the interleukin-6-induced epithelial-mesenchymal transition and metastasis through ROS production in hepatoma cells," *Cancer Letters*, vol. 421, pp. 1–14, 2018.
- [13] N. Ganne-Carrié, C. Chaffaut, V. Bourcier et al., "Estimate of hepatocellular carcinoma incidence in patients with alcoholic cirrhosis," *Journal of Hepatology*, vol. 69, no. 6, pp. 1274–1283, 2018.
- [14] W. Xue, S. Chen, H. Yin et al., "CRISPR-mediated direct mutation of cancer genes in the mouse liver," *Nature*, vol. 514, no. 7522, pp. 380–384, 2014.
- [15] S. Q. Li, D. M. Wang, S. Zhu, H. Y. Meng, H. M. Han, and H. J. Lu, "The protective roles of IL-6 trans-signaling regulated by ADAM9 on the liver in carbon tetrachloride-induced liver injury in mice," *Journal of Biochemical and Molecular Toxicology*, vol. 29, no. 7, pp. 340–348, 2015.
- [16] S. Q. Li, S. Zhu, H. M. Han, H. J. Lu, and H. Y. Meng, "IL-6 trans-signaling plays important protective roles in acute liver injury induced by acetaminophen in mice," *Journal of Biochemical and Molecular Toxicology*, vol. 29, no. 6, pp. 288–297, 2015.
- [17] S. Zargar, N. J. Siddiqi, S. K. Al Daihan, and T. A. Wani, "Protective effects of quercetin on cadmium fluoride induced oxidative stress at different intervals of time in mouse liver," *Acta Biochimica Polonica*, vol. 62, no. 2, pp. 207–213, 2015.
- [18] F. Zhao, J. Zhao, L. Song, Y. Q. Zhang, Z. Guo, and K. H. Yang, "The induction of apoptosis and autophagy in human hepatoma SMMC-7721 cells by combined treatment with vitamin C and polysaccharides extracted from *Grifola frondosa*," *Apoptosis*, vol. 22, no. 11, pp. 1461–1472, 2017.
- [19] H. Hui, W. Ma, J. Cui et al., "Periodic acid-Schiff staining method for function detection of liver cells is affected by 2% horse serum in induction medium," *Molecular Medicine Reports*, vol. 16, no. 6, pp. 8062–8068, 2017.
- [20] Y. Fu, J. D. Sander, D. Reyon, V. M. Cascio, and J. K. Joung, "Improving CRISPR-Cas nuclease specificity using truncated guide RNAs," *Nature Biotechnology*, vol. 32, no. 3, pp. 279–284, 2014.
- [21] B. P. Kleinstiver, M. S. Prew, S. Q. Tsai et al., "Engineered CRISPR-Cas9 nucleases with altered PAM specificities," *Nature*, vol. 523, no. 7561, pp. 481–485, 2015.
- [22] S. Zargar, T. A. Wani, A. A. Alamro, and M. A. Ganaie, "Amelioration of thioacetamide-induced liver toxicity in Wistar rats

- by rutin," *International Journal of Immunopathology and Pharmacology*, vol. 30, no. 3, pp. 207–214, 2017.
- [23] S. Gao, S. Li, X. Duan et al., "Inhibition of glycogen synthase kinase 3 beta (GSK3 $\beta$ ) suppresses the progression of esophageal squamous cell carcinoma by modifying STAT3 activity," *Molecular Carcinogenesis*, vol. 56, no. 10, pp. 2301–2316, 2017.
- [24] F.-M. Shang, S.-Q. Li, H.-J. Lu et al., "Expression changes of hepatic glycogen in mice with alcohol-induced liver injury," *The Chinese Journal of Clinical Pharmacology*, vol. 32, pp. 818–820, 2016.
- [25] L.-L. Wang, S.-Q. Li, H.-J. Lu et al., "Significance of expression of heat shock protein 70 in alcoholic liver injury in mice," *World Chinese Journal of Digestology*, vol. 24, pp. 2869–2874, 2016.
- [26] W. He, J. Feng, Y. Zhang, Y. Wang, W. Zang, and G. Zhao, "microRNA-186 inhibits cell proliferation and induces apoptosis in human esophageal squamous cell carcinoma by targeting SKP2," *Laboratory Investigation*, vol. 96, no. 3, pp. 317–324, 2016.
- [27] S. Gao, M. Zhang, X. Zhu et al., "Apoptotic effects of photofrin-Diomed 630-PDT on SHEEC human esophageal squamous cancer cells," *International Journal of Clinical and Experimental Medicine*, vol. 8, no. 9, pp. 15098–15107, 2015.
- [28] C. P. Li, J. H. Li, S. Y. He, P. Li, and X. L. Zhong, "Roles of Fas/Fasl, Bcl-2/Bax, and Caspase-8 in rat nonalcoholic fatty liver disease pathogenesis," *Genetics and Molecular Research*, vol. 13, no. 2, pp. 3991–3999, 2014.
- [29] Z. Kelman, "PCNA: structure, functions and interactions," *Oncogene*, vol. 14, no. 6, pp. 629–640, 1997.
- [30] J. M. Kim, H. G. Kim, J. M. Han et al., "The herbal formula CGX ameliorates the expression of vascular endothelial growth factor in alcoholic liver fibrosis," *Journal of Ethnopharmacology*, vol. 150, no. 3, pp. 892–900, 2013.
- [31] J. Zhao, Y. F. Qi, and Y. R. Yu, "STAT3: a key regulator in liver fibrosis," *Annals of Hepatology*, vol. 21, article 100224, 2021.